ELSEVIER

Solar Energy Materials & Solar Cells 59 (1999) 255–264

Solar Energy Materials & Solar Cells

www.elsevier.com/locate/solmat

Na incorporation in Mo and $CuInSe_2$ from production processes

A. Rockett[a,*], K. Granath[a,1], S. Asher[b], M.M. Al Jassim[b], F. Hasoon[b], R. Matson[b], B. Basol[c], V. Kapur[c], J.S. Britt[d,2], T. Gillespie[e], C. Marshall[e]

[a]*College of Engineering, University of Illinois, 1-107 ESB, 1101 W. Springfield Avenue, Urbana, IL 61801, USA*
[b]*National Renewable Energy Laboratory, 1617 Cole Boulevard, Golden, CO, USA*
[c]*ISET Inc., 8635 Aviation Boulevard, Inglewood, CA 90301, USA*
[d]*Energy Photovoltiacs Inc., P.O. Box 7456, Princeton, NJ 08543, USA*
[e]*Lockheed Martin Astronautics (LMA), P.O. Box 179, Denver, CO 80201, USA*

Received 14 January 1999; received in revised form 10 March 1999

Abstract

Results of characterization of thin films of Mo deposited by DC magnetron sputtering on soda-lime glass (Mo/SLG) and $CuInSe_2$ (CIS) on Mo/SLG are presented. The primary objective of the work was to clarify the factors determining the concentration of Na in commercial-grade CIS. Mo films were deposited by three laboratories manufacturing CIS thin film solar cells. Analysis was by secondary ion mass spectrometry, scanning electron microscopy and X-ray diffraction. Changes in Mo deposition parameters in general affected the Na level but there was no obvious link to any single Mo deposition parameter. Oxygen content directly affected the Na level. The Na behavior was not obviously connected to film preferred orientation. Selenization of the Mo layers was also examined. Elemental Se vapor was found to produce significantly less selenization than H_2Se. The amount of selenization was also strongly dependent upon Mo deposition conditions, although a specific source of the change in reaction rate was not found. Na distributions in the CIS deposited on the Mo were not limited by the diffusivity of the Na. The Na concentration in the CIS was increased by annealing the Mo films both with and without intentionally added Na. The Na level in the CIS appears to be set more by the CIS deposition process than by the Na concentration in the Mo so long as the Mo contains sufficient Na to

* Corresponding author. Tel.: 1-217-333-0417; fax: 1-217-244-1631.
E-mail address: arockett@staff.uiuc.edu (A. Rockett)
[1] Permanent address: Ångström Solar Center, Uppsala University, Uppsala, Sweden.
[2] present address: Global Solar Energy, 5575 South Houghton Rd., Tucson, AZ 85747, USA.

PII: S0927-0248(99)00026-4

saturate the available sites in the CIS.

Keywords: $CuInSe_2$; Photovoltaics; Na; Mo

1. Introduction

Large-scale production of $CuInSe_2$ (CIS)-based solar cells and modules requires a reproducible deposition process yielding high-quality material. To design and control such a process, it is of particular interest to know how process variables affect solar cell performance. Impurities, both beneficial and detrimental, may be incorporated into the device layers during fabrication of solar cells. CIS-based devices deposited by all common techniques have been found to show significant improvements when Na is present during formation of the CIS absorber [1–5]. Most studies of device performance as a function of impurity content have focused on CIS and Mo produced in laboratory-scale processes. It would be especially beneficial to know how Na is incorporated into the Mo back contact and the CIS absorber layers of solar cells fabricated by standard commercial techniques on soda-lime glass substrates and how it influences the properties of the CIS. In particular, it is important to know how critical the Na level in the Mo and the Mo deposition conditions are to the Na concentration in the CIS layer.

Previous works have considered the effects of Na incorporated into polycrystalline CIS layers grown by multiple source evaporation [1–4], selenization [5], and single-crystal epitaxial layers [6]. These results have suggested that Na is incorporated easily in sputtered Mo films. The Na resides primarily in the grain boundaries and does not move significantly in the grains of the Mo itself [7]. Further, it has been shown that the O concentration in the Mo plays a strong role in determining the Na content [7]. At least two groups have found evidence in the CIS of enhanced grain growth, increased (1 1 2) texturing and an increase in device performance when Na was present in the films [2,3]. Another study indicated that Na decreases the resistivity as well as the activation barrier to conduction in the plane of polycrystalline thin films of CIS [4]. This behavior was attributed to a decrease in the potential barriers at grain boundaries. Still others have found that Na increases the open-circuit voltage of polycrystalline devices and reduces the depletion width [1]. This may be linked to the observed Na-induced reductions in compensation in CIS [6].

The focus of the current work is determination of the dominant factors controlling the concentration of Na in CIS thin films. This work extends the previous results to commercial device-grade Mo and CIS layers. In particular we have examined the behavior of Na in the Mo and CIS as a function of the Mo deposition conditions and the CIS formation process. The type of glass was the same for each Mo deposition process. We have studied selenization of the Mo layers by H_2Se and under Se vapor in vacuum. Finally, we have characterized the transfer of Na to the CIS films from the Mo layers. The work was performed as part of the National CIS Team efforts coordinated by the National Renewable Energy Laboratory (NREL) through the Thin Film PV Partnership Program.

2. Experimental

The Mo films used in this study were deposited by DC magnetron sputtering in the CIS solar cell process lines of International Solar Electric Technology (ISET), Energy Photovoltaics (EPV), and Lockheed Martin Astronautics (LMA). In each case, 30 cm × 30 cm × 3 mm thick soda-lime glass substrates were supplied by ISET. Mo depositions involved two or more passes in front of magnetron sputtering targets. The sputtering geometries and the deposition conditions used are listed in Table 1. After deposition, portions of the samples were cut and sent to the University of Illinois (UIUC) and NREL for analysis and treatment with Na compounds. Additional samples cut from the same Mo-metallized glass substrates were exposed to selenizing atmospheres or coated with CIS using standard processes at ISET and EPV. No Ga was included in the CIS layers examined here to simplify the analysis.

Direct selenization of the Mo layers at ISET consisted of heating in H_2Se to 450°C in 10 min followed by a 30-min soak and a rapid cool down. Selenization of Mo layers at EPV involved a 15-min heating time to 450°C with a 10-min soak in elemental Se vapor. The pressure was determined by the equilibrium vapor pressure of Se at 450°C. The ISET CIS growth process involves selenization of Cu–In metallic precursor layers in H_2Se gas as was used for the Mo selenizations. The EPV process uses selenization of metallic precursors on a selenide compound in a vacuum environment with elemental Se vapor as above for the Mo. The selenization conditions using Se and H_2Se provide significantly different reaction pathways. Furthermore, the "thermal budget" of the EPV process is somewhat lower than for the ISET process.

Mo-coated glass samples were analyzed by scanning electron microscopy (SEM) at NREL and UIUC and by X-ray diffraction (XRD) in a Rigaku D-MAX diffractometer and by secondary ion mass spectrometry (SIMS) in a Cameca IMS-5f at UIUC. Additional XRD data was obtained at NREL. CIS-coated samples were analyzed at NREL by SIMS in Cameca IMS-5f or 3f instruments. The XRD measurements used Cu K_α radiation in all cases. SIMS measurements used Cs^+ or O_2^+ primary ion beams. Measurements of both positive and negative secondary ions were made in some cases although data presented below are for positive secondary ions.

3. Results

3.1. Na in Mo

As-deposited Mo soda-lime glass substrates (Mo/SLG) were examined by fracture-cross-section scanning electron microscopy (XSEM), SIMS (Fig. 1), and XRD (Fig. 2). All films had a $\langle 1\,1\,0 \rangle$ preferred orientation, as expected for a sputter-deposited bcc metal deposited on an amorphous substrate. They exhibit columnar microstructures with column diameters of ~ 30 nm as determined by XSEM. A distinct ripple in the columns was observable due to the samples passing across the face of the sputtering source and thus experiencing a variation in the direction of the source material with time. Boundaries were found with new column nucleation occurring at the end of each pass by the target. All samples contained significant quantities of O and Na. While the

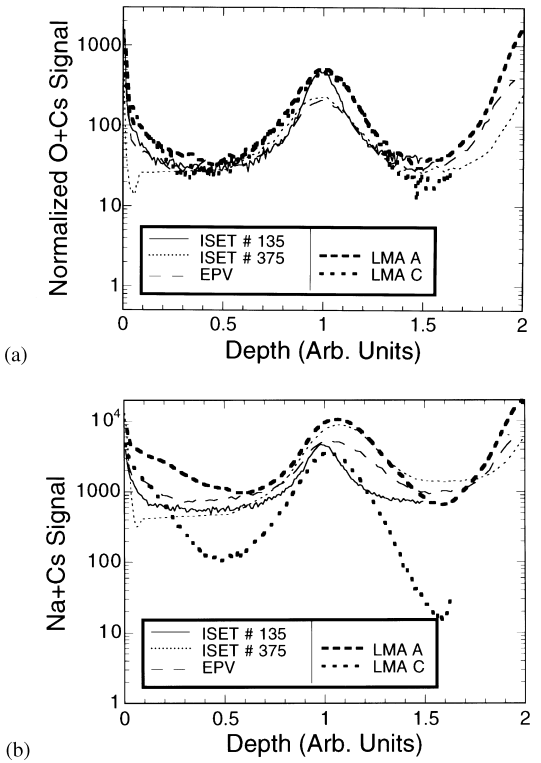

Fig. 1. An overlay of Mo SIMS depth profiles for (top) oxygen and (bottom) sodium. Oxygen signals have been divided by the base pressure of the deposition system (from Table 1). Positively charged complexes with Cs were monitored to minimize analysis artifacts.

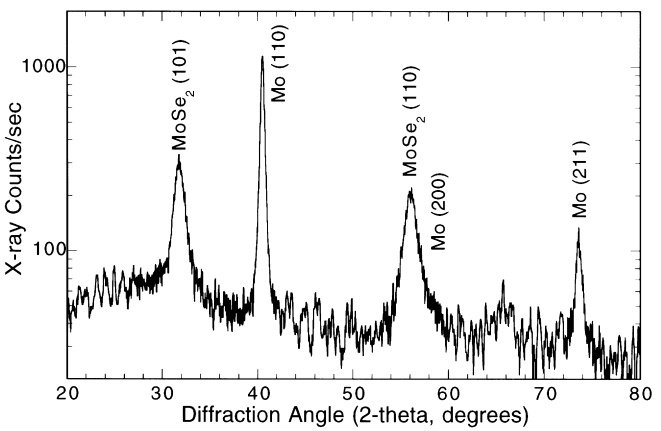

Fig. 2. XRD results for the LMA A Mo layer after H_2Se selenization.

Na content in the Mo layers did not track the O content exactly, the ratio of the O signal to the Na signal was relatively constant within a given sample. The oxygen profiles were identical, within the error of the SIMS analysis, after normalizing the signals to the oxygen partial pressure during deposition (see Fig. 1a). We conclude that the oxygen in each Mo layer was due to residual gas in the deposition system. The Na presumably came from the soda-lime glass substrate.

During each deposition the sample passed from one extreme end to the other of the sputtering target. Hence, the initial and final deposition rates were relatively low and the flux of energetic particles hitting the Mo film should have been relatively high. At the end of each deposition cycle, oxygen contamination from the chamber was relatively high as compared to when the substrate was directly beneath the target because of the low deposition rate at the end of each cycle. In addition, the grain size in the end-of-pass regions was found to be small which might also have increased the incorporation probability of oxygen. Strong peaks in the O and Na signals were observable in the SIMS profiles at these boundaries (Fig. 1). Indeed, the ratio of O-to-Mo SIMS counts at the boundaries is approximately equal to the ratio observed for MoO_3 deposited by reactive RF sputtering of Mo in oxygen gas. This suggests that the boundaries were completely oxidized.

XRD spectra were fit with Gaussian curves to determine the peak positions, full-width at half-maximum, and areas. The results of fits to some of the peaks are given in Table 1. There are no obvious relationships between variations in the sputtering parameters and variations in the XRD results. This is not surprising as most deposition parameters varied among the processes tested here. Because most parameters interact, the state of stress and microstructure of the films would not be simply related to any one parameter.

Each 30 cm × 30 cm × 3 mm Mo-coated glass substrate was cut into a number of smaller samples. One of these samples was dipped in an $NaHCO_3$ solution and

Table 1
Mo deposition conditions

Source	Units	ISET	ISET	LMA	LMA	EPV
Sample number		135	375	A	C	
Base pressure	$\times 10^{-6}$ Torr	5	1.5	0.76	0.38	2.1
Sputtering pressure	mTorr	8	6	9	5	1.0
Power density	W/cm^2	13	25	19	19	3.7
Source-to-substrate distance	cm	4	4	7.4	7.4	5
Pretreatment		350°C	None	None	None	None
Thickness	μm	2.2	0.5	0.5	1	0.5
Average deposition rate	nm/s	0.4	1.3	1	0.8	0.5
Passes by the target		4	2	2	2	3
Transport speed	cm/min	1.8	16.2	4.9	2.04	15.4
$MoSe_2$ layer thickness (SIMS)	μm	0.05	Failed	0.29	0.58	0.1 6
$MoSe_2$ layer thickness (XRD)	arb. units	0.004	0.99	0.28	0.34	0.04
(1 1 0) Mo 2θ peak position	deg	40.46	40.60	40.53	40.60	–
(1 1 0)/(1 1 2) Mo peak ratio		23	8.5	11	16	6.1
(1 0 0)/(1 1 0) $MoSe_2$ peak ratio		3.2	0.3	1.5	2.0	1.0

allowed to dry, leaving a bicarbonate coating on the surface. Another sample was coated with a thin layer of Na_2Se by evaporation. A third sample was not treated with an Na compound and served as a standard for comparison. After annealing in vacuum at 450°C for 20 min (chosen to be similar to selenization conditions), these three samples were reanalyzed by SIMS. All had approximately equal Na contents and profiles through their thickness were nearly identical in shape to the as-deposited material. However, the signal had increased by one order of magnitude indicating significantly more Na in all annealed materials compared to the as-deposited samples. The oxygen contents and depth profiles were unchanged with this anneal. The Na concentration in the films was not limited by the availability of Na because the samples heat-treated with and without surface-Na showed similar results. This indicates that sufficient Na can come from the substrate glass to provide Na to the Mo. Furthermore, the profiles show both increases and decreases in Na content with depth indicating that diffusion was driven by the presence of oxides and the structure of the Mo and not by an Na concentration gradient. XRD peak position and consequently the Mo lattice constant were weakly related to O content in the films. Lower O contents were typically associated with smaller Mo lattice constants.

Pieces of each Mo-coated glass sample were selenized at ISET in H_2Se gas and at EPV in elemental Se vapor at 450°C. The elemental Se produced a barely detectable selenization of all of the Mo layers that were examined. The H_2Se treatment, on the other hand, selenized the different Mo samples to different but clearly measurable extents (see Fig. 3). The approximate thicknesses of the selenized layers are given in

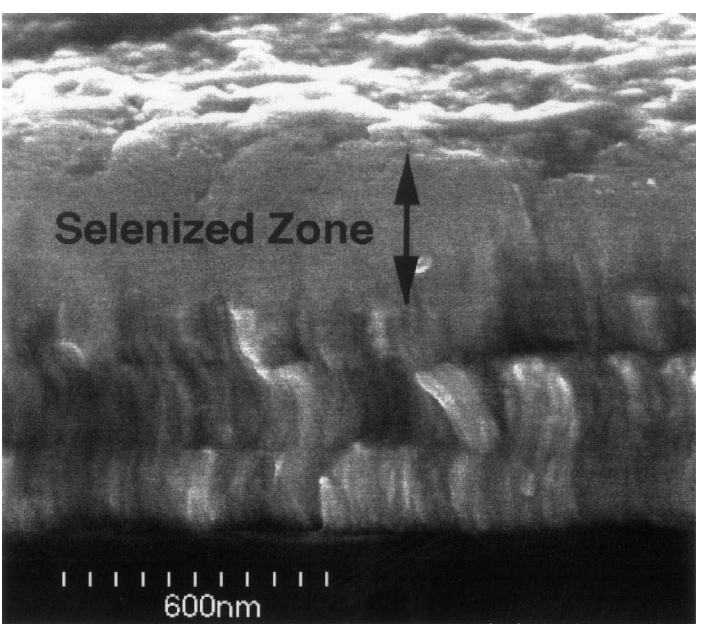

Fig. 3. A fracture-cross-section scanning electron micrograph of the Mo 135 sample deposited at ISET and selenized in H_2Se. Boundaries within the layer occurred at the end of each sputtering cycle.

Table 1. The $MoSe_2$ formed had a preferred orientation, which increased as the preferred orientation of the Mo increased (compare values in Table 1). A clear difference in the susceptibility of the layers to selenization is evident, although the amount of selenization could not be directly related to the microstructure or deposition conditions. Thus, the cause of the variability in the selenization rate is not clear. It presumably resulted from changes in the grain structure in the films. After H_2Se selenization, SIMS analysis showed an increase in Na in the films equivalent to (in the case of the ISET 375 samples) or greater than (for the ISET 135 and EPV samples) the change during annealing at 450°C. O levels were unchanged by selenization in the bulk of the samples. Relatively little oxygen was found in the selenized regions.

In summary, the results show no clear trends with Mo deposition conditions but oxygen content and possibly (at least indirectly) Mo grain boundary volume has a significant effect on Na incorporation in the Mo.

3.2. Na in CIS

Mo/SLG samples cut from the same substrates used for the Mo analyses were coated with CIS at ISET and EPV. SIMS analyses were then performed at NREL on the completed structures. Typical SIMS profiles for the complete structures with CIS deposited at EPV and ISET on the ISET 135 Mo sample are shown in Fig. 4. Profiles for other samples are qualitatively very similar to the profiles shown. Fig. 5 compares Na profiles for the CIS deposited at EPV for three of the Mo samples tested. The most apparent result that can be seen by comparing the Na levels in Figs. 4 and 5 is that the average concentration and profile of Na in the CIS depends much more strongly on the CIS deposition process than on the Mo underlying it in the samples studied here[3]. The Na levels in the CIS deposited at ISET were virtually identical for all samples except for the sample on ISET 375 which had less Na at the rear and more at the front of the CIS. The EPV CIS samples showed significantly more variation, up to a factor of eight, in Na concentration although the shapes of the profiles were still almost identical. The Na level in the EPV CIS films varied somewhat, as can be seen in Fig. 5, due to differences in the Na level in the Mo but this effect was smaller than the change due to the CIS deposition process differences from EPV to ISET. Overall, the EPV samples exhibited almost an order of magnitude less Na near the CIS surface and a thinner, less consistent region of enhanced Na concentration near the Mo interface (see Fig. 4a). This may have been related to the lower thermal budget of the EPV process or to the different selenization chemistry.

The most likely explanation for the observation of increased Na concentration near the back of the CIS film is that Na content may be controlled by the microstructure of the CIS. It is known that all CIS films formed by selenization of metal layers have smaller grain sizes near the back of the films (and verified for films studied here by XSEM). Furthermore, it has been found that Na tends to accumulate in these regions. Evidence has also been found for Na segregation out of CIS layers to surrounding

[3] For a detailed study of the effect of Na precursors on the Na level in evaporated CIGS, see Ref. [8].

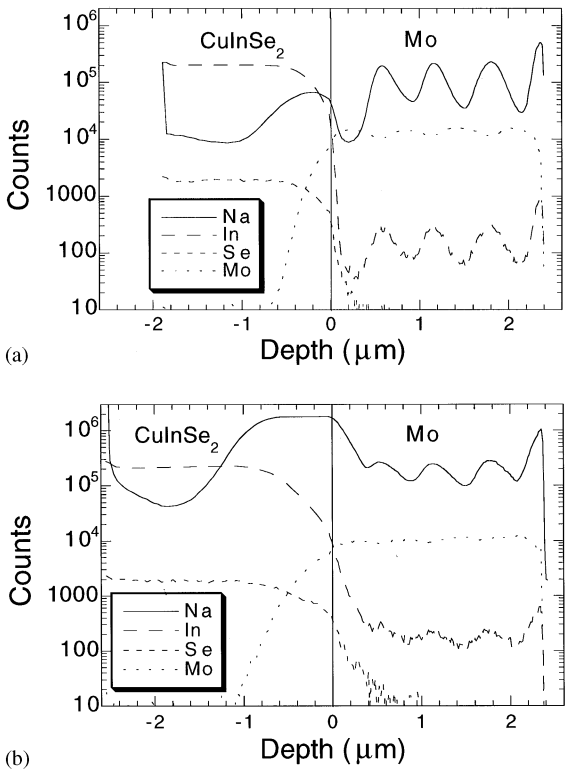

Fig. 4. Typical SIMS profiles for the complete structures with CIS deposited at a) EPV and (b) ISET and using the ISET 135 Mo. The results show that for the same Mo layer and the same selenization time and temperature the ISET H_2Se process causes more Na to diffuse into the CIS than for the EPV Se process. The Na signal in (b) was limited at the maximum by detector counting rate. The true signal level probably exceeded 2×1^6.

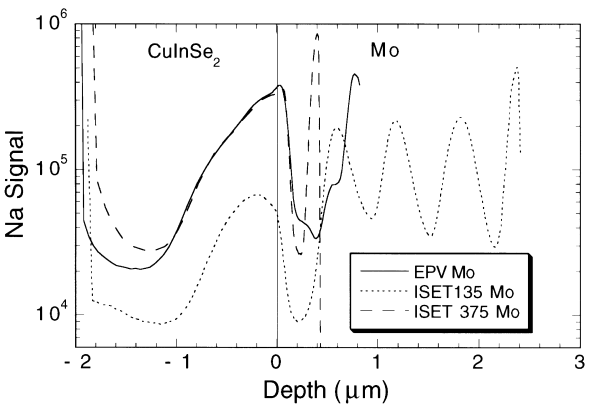

Fig. 5. Compares Na profiles for the CIS deposited by selenization of metals in an Se vapor at EPV on three different Mo samples. Sources of Mo are given in the figure legend.

interfaces in some cases [9]. The observed profile is consistent with segregation of Na toward the back of the film during selenization. Experiments currently in progress will examine partially reacted layers to further evaluate these potential mechanisms. Depth profiles have shown little oxygen present in the CIS indicating that the observed behavior of Na is not the result of an interaction with O.

4. Conclusions

Na is incorporated into the Mo layers apparently from the soda-lime glass to a level which is not strongly correlated with the Mo deposition process and with little relation to the crystallography of the Mo as determined by XRD. It appears that the primary effect is the oxygen concentration with a possible secondary relation to grain boundary volume or effective surface area in the Mo film. This is not measured directly by XRD and is a complex function of deposition conditions. This explains the variation from sample to sample with large changes in process conditions. Some of the Na in the Mo layer then moves into the CIS, when deposited by the techniques used here, to a level strongly dependent on the CIS process conditions and only weakly related to the Mo properties. The Mo influences the supply of Na, not the density of available sites for Na in the CIS. Thus if the system is limited by the supply of Na, then the Na level in the Mo has a significant impact on the Na level in the CIS. However, if the Na level in the Mo is sufficiently high, then the Na level in the CIS is relatively independent of the concentration in the Mo. (This is apparently the case of the ISET Mo samples.) Compare also the two profiles in Fig. 4 which have identical Mo layers but very different Na in the CIS films. We conclude that the most likely explanation for the observations is that the Na level is correlated with grain size in the Mo, probably because that is where oxygen is located. Selenization of the Mo varies significantly from one process to another but is not simply related to deposition conditions. Elemental Se vapor was found to produce significantly less selenization than H_2Se.

5. For further reading

The following reference is also of interest to the reader: [8]

Acknowledgements

The authors gratefully acknowledge the support of the National Renewable Energy Laboratory under the Thin Film PV Partnership and Universities programs. The advice and comments of the remainder of the CIS team are also appreciated. Lockheed Martin Astronautics (LMA) participation was funded by combined LMA Internal Research and Development Project D-90, Advanced Structures and Materials, and under DARPA agreement number MDA972-95-3-0036.

References

[1] M. Ruckh, D. Schmid, M. Kaiser, R. Schäffler, T. Walter, H.W. Schock, Proceedings of the First World Conference on Photovoltaic Energy Conversion, IEEE, New York, 1994, p. 156.
[2] M. Bodegård, L. Stolt, J. Hedström, Proceedings of the 12th European Photovoltaic Solar Energy Conference, Amsterdam, H.S. Stephens and Assoc., April 1994, p. 1743.
[3] V. Probst, J. Rimmasch, W. Riedl, W. Stetter, J. Holz, H. Harms, F. Karg, Proceedings of the First World Conference on Photovoltaic Energy Conversion, IEEE, New York, 1994, p. 144.
[4] J. Holz, F. Karg, H. von Philipsborn, Proceedings of the 12th European Photovoltaic Solar Energy Conference, Amsterdam, H.S. Stephens & Assoc., April 1994 p.1592.
[5] U. Rau, M. Schmitt, D. Hilburger, F. Engelhardt, O. Seifert, J. Parisi, Proceedings of the 25th IEEE Photovoltaic Specialists Conference, IEEE, New York, 1996, p. 1005.
[6] D.J. Schroeder, A.A. Rockett, J. Appl. Phys. 82 (10) (1997) p. 4982.
[7] K. Granath, L. Stolt, M. Bodegård, A. Rockett, D.J. Schroeder, Proceedings of the 14th European Photovoltaic Solar Energy Conference, Barcelona, 30 June–4 July 1997 H.S. Stephens & Assoc., p. 1278.
[8] M. Bodegård et al., Proceedings of the 13th European Photovoltaic Solar Energy Conference, Nice, Nice, H.S. Stephens and Assoc., 23–27 October 1995, p. 2080.
[9] A. Rockett, M. Bodegård, K. Granath, L. Stolt, Proceedings of the 25th IEEE Photovoltaic Specialists Conference, Washington, DC, Institute of Electrical and Electronics Engineers, New York, May 1996, p. 985.